# Phase separation and suppression of critical dynamics at quantum phase transitions of MnSi and (Sr1−xCax)RuO3

**Article** *in* Nature Physics · December 2006

DOI: 10.1038/nphys488 · Source: OAI

CITATIONS
137

READS
467

**21 authors**, including:

Jeremy P. Carlo
Villanova University
**53** PUBLICATIONS **1,195** CITATIONS
SEE PROFILE

A. T. Savici
Oak Ridge National Laboratory
**125** PUBLICATIONS **2,617** CITATIONS
SEE PROFILE

Adam Aczel
Oak Ridge National Laboratory
**166** PUBLICATIONS **2,968** CITATIONS
SEE PROFILE

Jg Rodriguez
University Center CIFE
**405** PUBLICATIONS **13,379** CITATIONS
SEE PROFILE

# Phase separation and suppression of critical dynamics at quantum phase transitions of MnSi and $(Sr_{1-x}Ca_x)RuO_3$

Y. J. UEMURA[1]*, T. GOKO[1,2], I. M. GAT-MALUREANU[1,3], J. P. CARLO[1], P. L. RUSSO[1], A. T. SAVICI[1], A. ACZEL[4], G. J. MACDOUGALL[4], J. A. RODRIGUEZ[4], G. M. LUKE[4], S. R. DUNSIGER[4], A. MCCOLLAM[5], J. ARAI[2], CH. PFLEIDERER[6], P. BÖNI[6], K. YOSHIMURA[7], E. BAGGIO-SAITOVITCH[8], M. B. FONTES[8], J. LARREA[8], Y. V. SUSHKO[9] AND J. SERENI[10]

[1]Department of Physics, Columbia University, New York, New York 10027, USA
[2]Department of Physics, Tokyo University of Science, Noda, Chiba 278-8510, Japan
[3]Department of Science, SUNY Maritime College, Throggs Neck, New York 10465, USA
[4]Department of Physics and Astronomy, McMaster University, Hamilton, Ontario L8S 4M1, Canada
[5]Department of Physics, University of Toronto, Toronto, Ontario M5S 1A7, Canada
[6]Physik Department, Technische Universität München, D-85748 Garching, Germany
[7]Department of Chemistry, Kyoto University, Kyoto 606-8502, Japan
[8]Centro Brasilieiro de Pesquisas Fisicas, Rua Xavier Sigaud 150 Urca, CEP 22290-180 Rio de Janeiro, Brazil
[9]Department of Physics and Astronomy, University of Kentucky, Lexington, Kentucky 40506-0055, USA
[10]Laboratorio de Bajas Temperaturas, Centro Atomico Bariloche, 8400 San Carlos de Bariloche, Argentina
*e-mail: tomo@lorentz.phys.columbia.edu

Published online: 24 December 2006; doi:10.1038/nphys488

**Quantum phase transitions (QPTs) at zero temperature are generally studied by means of pressure or composition tuning. Volume-integrated probes such as neutron and magnetization measurements, as well as pressure uncertainties in NMR studies using powder specimens, however, have limited the characterization of magnetism and detection of discontinuous changes at QPTs. Overcoming these limitations, we carried out muon spin relaxation measurements that have a unique sensitivity to volume fractions of magnetically ordered and paramagnetic regions, and studied QPTs from itinerant helimagnet or ferromagnet to paramagnet transitions in MnSi (single crystal; varying pressure) and $(Sr_{1-x}Ca_x)RuO_3$ (ceramic specimens; varying $x$). Our results provide the first clear evidence that both cases are associated with phase separation and suppression of dynamic critical behaviour, reveal slow dynamics of the 'partial order' diffuse spin correlations in MnSi above the critical pressure and suggest the possibility that a majority of QPTs in correlated electron systems involve first-order transitions and/or phase separation.**

Advances in materials preparation and characterization techniques have revealed complicated and sometimes unexpected phenomena near phase transitions and phase boundaries in correlated electron systems. Fascinating examples can be found in pressure-tuned changes from ferromagnetic (or helimagnetic) to paramagnetic states in itinerant electron systems, such as MnSi (refs 1,2) and $ZrZn_2$ (ref. 3), as well as $UGe_2$ (ref. 4), which are associated with the appearance of a superconducting state near the disappearance of ferromagnetism. MnSi exhibits magnetic order with a spontaneous ordered moment $m_s(T \to 0) = 0.4$ Bohr magneton per Mn and a long-period (180 Å) helical modulation below the magnetic ordering temperature $T_c = 29.5$ K at ambient pressure[5]. This system has been extensively studied as a prototypical weak itinerant magnet existing near the boundary of disappearance of metallic ferromagnetism in the evolution from Fe, Ni or MnSi, to the correlated paramagnet Pd, with a decreasing degree of localized moment character and decreasing ordered moment size $m_s$ relative to the effective paramagnetic moment, $m_p^{eff}$ (ref. 6, and references therein).

Magnetic order in MnSi can be suppressed by application of hydrostatic pressure $p$ above the critical pressure $p_c = 14.6$ kbar (ref. 1). Discontinuous changes in the magnetic susceptibility observed between $p^* = 12$ kbar and $p_c$ suggest a first-order thermal phase transition at $T_c$ in a narrow pressure region before the disappearance of magnetic order. Recent neutron studies[2] have revealed the existence of 'partial order' spin correlations, extending over a wide pressure region at $p > p_c$ at low temperatures below $T_0$, whose diffusive intensity profile in reciprocal space is illustrated in Fig. 1a. The non-zero ordered moment size at $T \to 0$, measured by Si nuclear magnetic resonance (NMR)[7,8] up to $p = p_c$, indicates the disappearance of magnetism in the first-order transition as a function of $p$. The NMR intensity from magnetically ordered regions was found[8] to decrease with increasing $p$ at 12–17 kbar. Pressure inhomogeneity in powderized NMR specimens[8], however, prevented unambiguous determinations of (1) pressure regions with spatial heterogeneity and (2) the relationship of this phenomenon to the partial-order behaviour.

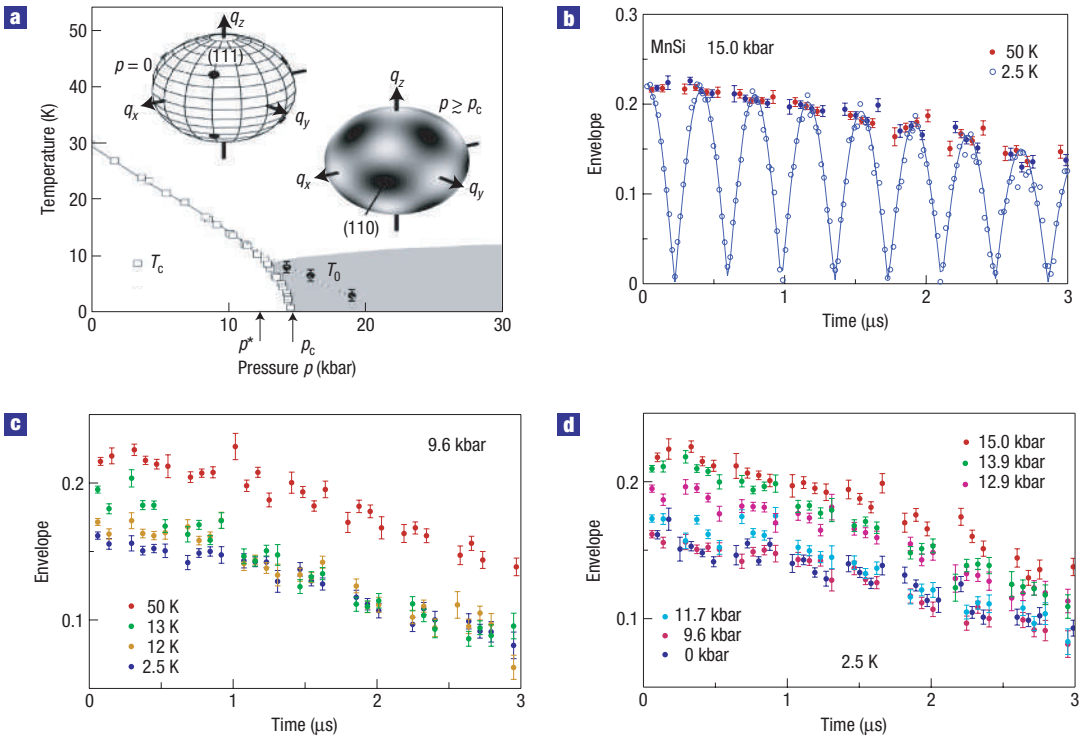


**Figure 1 Temperature–pressure phase diagram and envelope of μSR oscillation spectra of MnSi. a**, Phase diagram of MnSi as a function of pressure[2]. History-dependent behaviour has been found between $p^* \sim 12$ and $p_c = 14.6$ kbar. Diffuse neutron scattering intensity, illustrated in an intensity-map sphere (inset), was observed below $T_0$ (solid circles). Transport measurements exhibit non-Fermi-liquid behaviour in the shaded region. **b**, Muon spin precession pattern observed in a single-crystal specimen of MnSi within a pressure cell in a WTF of 100 G, and the envelope of the oscillation spectra. The amplitude of this envelope represents muons in the non-magnetic or paramagnetic environment. **c**, Temperature dependence of the envelope at $p = 9.6$ kbar. The reduction of the precessing envelope is caused by the volume of the specimen that has undergone static magnetic order. The envelope at $T = 2.5$ K represents muons stopped in the pressure cell. **d**, Pressure dependence of the envelope at $T = 2.5$ K. Static magnetic order takes place in 100% of the volume of MnSi at ambient pressure and 9.6 kbar, whereas in a reduced volume fraction between $p = 11.7$ and 13.9 kbar.

With its unique sensitivity to slow spin fluctuations and to signals both from paramagnetic and ordered volume fractions, muon spin relaxation[9,10] (μSR) is a probe well suited to shed new light on magnetic behaviours around quantum phase transitions (QPTs). Following earlier μSR studies of MnSi at ambient pressure[11–13], we explored the crossover region with $p = 10$–16 kbar using a single-crystal specimen in a standard piston-type pressure cell with a backward muon beam of momentum 103 MeV $c^{-1}$ from the M9 muon channel at the Canadian meson facility TRIUMF. Typically ~30% of the muons stopped in the specimen, of 6 mm in diameter and 10 mm in length, whereas 70% stopped in the wall of the pressure cell, of 23 mm in outer diameter. To assure temperature homogeneity, we used a gas-flow cryostat and two independent thermometers located at the top and bottom of the pressure cell, whose readings matched typically within ±0.1 K.

In single-crystal specimens of ordered magnetic systems, measurements in a weak transverse external field (WTF) are the best way to obtain μSR signals from a paramagnetic volume fraction. Figure 1b shows the precession signal and its envelope function observed in a WTF of 100 G at $p = 15$ kbar, $T = 50$ and 2.5 K. The technical details of processing μSR data are described in the Methods section. The nearly identical signal at these two temperatures indicates that 100% of the volume is paramagnetic at $T = 2.5$ K at this pressure. At $p = 9.6$ kbar, as shown in Fig. 1c, the envelope exhibits a clear reduction with decreasing temperature, caused by the missing signal from the magnetically ordered region of the specimen. The pressure dependence of the signal at $T = 2.5$ K in Fig. 1d shows that the volume fraction of the magnetically ordered region increases with decreasing pressure. From earlier μSR studies, it is known that 100% of the volume shows magnetic order below $T_c$ at ambient pressure with rather large internal fields (0.9 kG and 2.1 kG) at muon sites at low temperatures[12]. Thus, the envelope signals for $p = 0$ and 9.6 kbar in Fig. 1d represent muons that stopped in the pressure cell.

By subtracting this background signal from the observed envelope, we can obtain the WTF signal from the paramagnetic region of the specimen, from which the volume fraction, $V_f$, of the region with static magnetic order was derived. The temperature and pressure dependence of $V_f$ is shown in Fig. 2a,c. In the pressure region between $p = 11.7$ kbar ($\sim p^*$) and 13.9 kbar, the static magnetic order remains in a partial volume fraction at $T \to 0$, and the ordered region completely disappears at $p = 15$ kbar, which is slightly above $p_c = 14.6$ kbar. The frequency of the spontaneous muon spin precession from the magnetically ordered volume, determined in separate zero-field μSR measurements, remains finite below 13.9 kbar, as shown in Fig. 2c. These results indicate that the region between $p^*$ and $p_c$ is associated with phase separation between ordered and paramagnetic volumes, whereas there is no volume with static magnetism above $p_c$. Static magnetism with a Mn spin component $>0.004\,\mu_B$ per Mn, either in ferromagnetic or spin-glass-like correlations, would have produced a static internal magnetic field >10 G (significantly larger

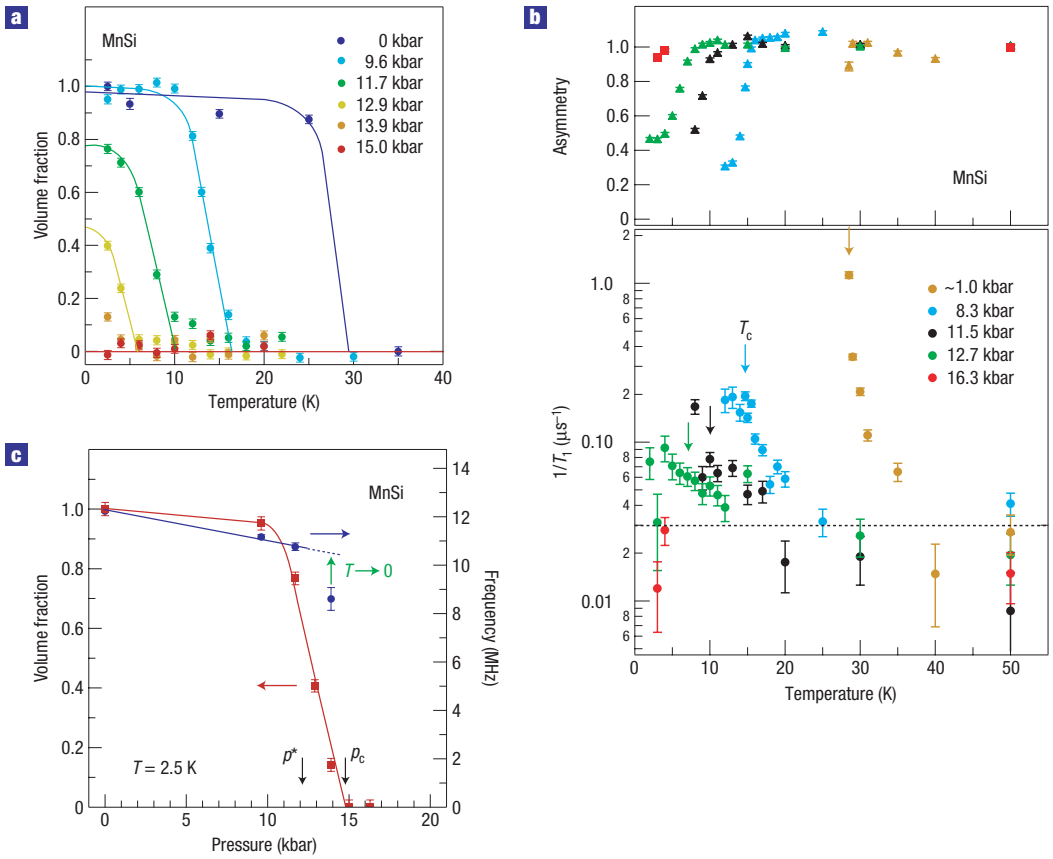


**Figure 2 μSR results on the volume fraction, relaxation rate and spin precession frequency in MnSi. a**, Temperature and pressure dependences of the volume fraction, $V_f$, with static magnetic order determined in WTF of 100 G. $V_f$ remains finite at $T \to 0$ at the pressure $p$ between 11.7 and 13.9 kbar, indicating phase separation between magnetically ordered and paramagnetic volumes. **b**, The muon spin relaxation rate $1/T_1$ and the relative magnitude of the corresponding muon asymmetry in MnSi in an LF of 200 G. Divergent critical behaviour of $1/T_1$, seen at $p \sim 1$ kbar, is gradually suppressed with increasing pressure. No anomaly of $1/T_1$ is seen at $T_c$ (indicated by arrows) at $p = 12.7$ kbar ($p^* < p < p_c$). At $p = 16.3$ kbar, $1/T_1$ becomes smaller than the technical limit of detection, indicated by the dashed line. **c**, Pressure dependence of $V_f$ and the zero-field muon spin precession frequency at $T = 2.5$ K. The finite frequency near $p_c$ indicates a first-order phase transition. The frequency at $p = 13.9$ kbar at $T = 2.5\,\text{K} \sim 0.5\,T_c$ is expected to increase for $T \to 0$ as illustrated by the green arrow.

than the nuclear dipolar fields ~4 G from Mn). This situation should have led to a distinguishable difference between $T = 50$ and 2.5 K data in Fig. 1b, and thus can be ruled out by the present data.

To study dynamic spin fluctuations, we also carried out measurements of the muon spin relaxation rate $1/T_1$ in a longitudinal field (LF) of 200 G. As shown in Fig. 2b, the relaxation rate at $p \sim 1$ kbar exhibits divergent behaviour, reproducing earlier results at ambient pressure[11–13]. The critical behaviour becomes less pronounced with increasing pressure. At $p = 12.7$ kbar between $p^*$ and $p_c$, the anomaly of $1/T_1$ at $T_c$ completely disappears, and the relaxation rate becomes smaller than our detection limit (dashed line in Fig. 2b) at $p_c < p$. In systems with magnetic order in a full volume fraction, the asymmetry of the LFμSR signal becomes 1/3 below $T_c$ as shown for the results at $p = 8.3$ kbar. The asymmetry at $p = 12.7$ kbar at $T \to 0$ is significantly larger than 1/3, indicating that the magnetic order occurs only in a partial volume fraction, thus confirming the results in WTF. The full amplitude LF signal at $p = 16.3$ kbar confirms that there is no magnetically ordered volume above $p_c$.

The absence of any observable relaxation puts a severe limit on the timescale of dynamic spin fluctuations of the 'partial order' spin correlations. To estimate the rate, $\nu$, of these fluctuations, we use the well-known formula, $1/T_1 \sim (\gamma_\mu \times H)^2/\nu$, where $H$ denotes the local field strength and $\gamma_\mu = 2\pi \times 1.36 \times 10^4\ \text{s}^{-1}\,\text{G}^{-1}$ is the gyromagnetic ratio of the muon spin. For a trial value of $H \sim 500$ G expected for the Mn spin polarization of $\sim 0.2\,\mu_B$, the lower limit of $\nu > 1.2 \times 10^{10}\ \text{s}^{-1}$ is given by the upper limit $1/T_1 < 0.15\ \mu\text{s}^{-1}$ indicated by the absence of relaxation in WTFμSR at $p = 15.0$ kbar and $T = 2.5$ K. Similarly, the (safe) upper limit $1/T_1 < 0.05\ \mu\text{s}^{-1}$, observed in LFμSR at 16 kbar and $T = 2.9$ K, indicates $\nu > 3.6 \times 10^{10}\ \text{s}^{-1}$. Although it is difficult to obtain a precise value of $H$ for the partial-order correlations, the above values serve as a reasonable estimate for the order of magnitude of $\nu$ from μSR. Neutron scattering signals from the partial order were detected in a quasi-elastic scan with an energy resolution of 50 μeV (ref. 2), which selects static (quasi-elastic) versus dynamic responses with a fluctuation rate of $10^{11}\ \text{s}^{-1}$. Thus, the combination of neutron and the present μSR results indicate that the 'partial order' spin correlations have dynamic character at a timescale between $10^{-11}$ and $10^{-10}$ s.

As an influence of the helical modulation in the case of MnSi might be expected, we also carried out μSR measurements in the metallic system $(Sr_{1-x}Ca_x)RuO_3$ at ambient pressure, using ceramic specimens and a surface muon beam at TRIUMF. The unsubstituted $SrRuO_3$ exhibits ferromagnetic order with $T_c \sim 160$ K and an ordered moment $m_s \sim 0.8\,\mu_B$ per Ru at

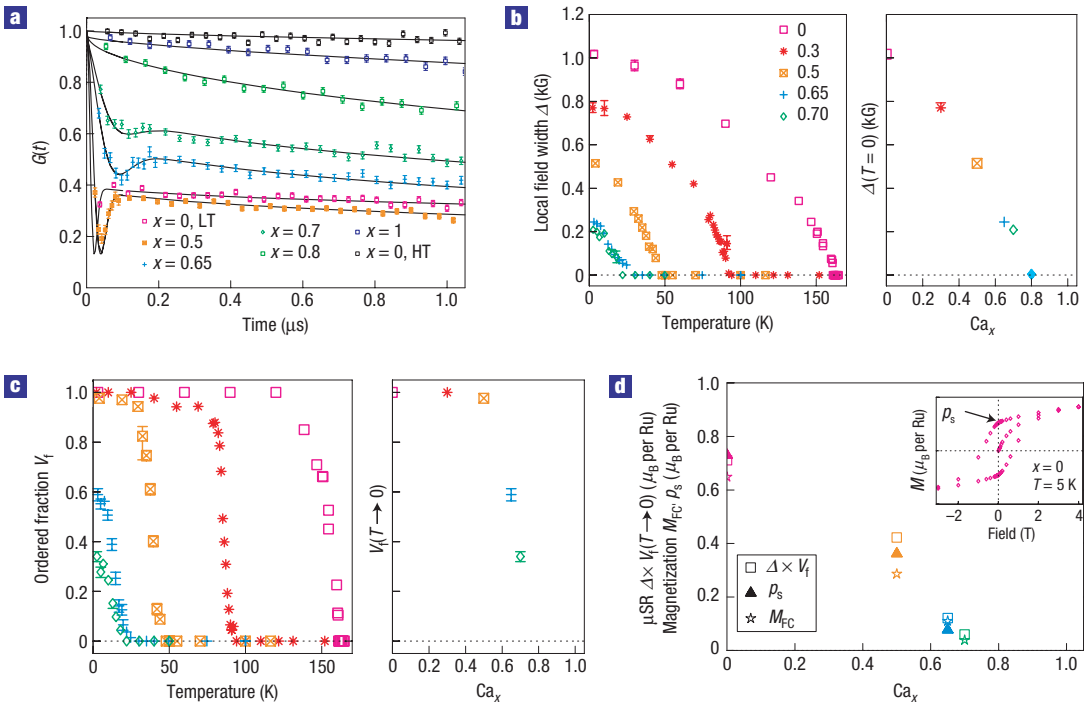


**Figure 3 ZF μSR and magnetization results in $(Sr_{1-x}Ca_x)RuO_3$.** **a**, μSR spectra observed at $T \sim 2.5-5$ K (indicated as LT) in ceramic specimens of various $x$ and at $T = 164$ K (HT) in $SrRuO_3$ above $T_c$. The LT spectra show a damped oscillation with the amplitude of 2/3, expected for static order in full volume, in $x = 1.0$ and 0.5. A reduced amplitude for $x = 0.65$ and 0.7 indicates a finite volume fraction of magnetically ordered region. A slow relaxation for $x > 0.7$ suggests disappearance of the volume with ordered moment greater than $m_s \sim 0.01\ \mu_B$ per Ru. The solid line represents a fit to a gaussian Kubo–Toyabe function multiplied by an exponential decay. **b**, The gaussian width, $\Delta$, of the static random local field obtained in this fitting for different doping levels $x$. $\Delta$ is proportional to the average size of static ordered moment in the magnetically ordered volume. **c**, Volume fraction, $V_f$, of the magnetically ordered region, derived from ZF μSR (same colour key as **b**). **d**, Comparison of $\Delta \times V_f(T \to 0)$ by μSR with the magnetization measured in field cooling, ($M_{FC}$), and the spontaneous moment, $p_s$, seen in the field-cycling, as illustrated in the inset, all measured at low temperatures (2–5) K. $M_{FC}$ and $p_s$ represent the volume-integrated responses. Same colour key as **b**.

$T \to 0$. With increasing Ca concentration $x$, both $T_c$ and $m_s$ decrease, and ferromagnetic order disappears at $x \sim 0.7$, whereas the paramagnetic effective moment $m_p^{eff} \sim 3.0\ \mu_B$ per Ru remains nearly unchanged between $x = 0$ and 1 (refs 14,15). This is the typical behaviour expected from the self-consistent renormalization theory of Moriya and co-workers developed for weak ferromagnetism of itinerant electron systems (ref. 6, and references therein). Figure 3a shows time spectra of the muon spin polarization observed in zero field at $T \sim 2$ K for specimens with various Ca concentrations. For $x = 0$ and 0.5, we see a fast damped oscillation of 2/3 of the asymmetry followed by a slowly relaxing 1/3 component, which is expected for systems with magnetic order in 100% of the volume. The absence of long-lived muon precession is due to magnetic domain structures in ceramic specimens. The spectra for $x = 0.65$ and 0.7 exhibit a slower damped oscillation, followed by an increased slow-decay component, indicating that the magnetic order occurs in a partial volume fraction. No clear signature of magnetic order can be seen for $x = 0.8$ and 1.0 systems.

Figure 3b shows the local field width, $\Delta$, derived from the damped oscillation signal, which is proportional to the ordered moment within the magnetically ordered volume. More data for around $x = 0.7$ are needed to determine whether $\Delta(T \to 0)$ changes abruptly or continuously as a function of $x$. The volume fraction, $V_f$, of the magnetically ordered region is shown in Fig. 3c, which clearly demonstrates phase separation between ordered and paramagnetic regions within a narrow concentration range before the disappearance of ferromagnetism. The product of the local moment size and the volume fraction, shown in Fig. 3d, scales with bulk magnetization, which reflects the volume-integrated quantity. We have also carried out $1/T_1$ measurements in zero-field (ZF) μSR in $(Sr_{1-x}Ca_x)RuO_3$. The slope of $T_1$ versus $1/T$ above $T_c$, which signifies the strength of the critical divergence of the relaxation rate[11,13], is reduced with increasing $x$ and becomes nearly 0 at $x \sim 0.7$, indicating that the dynamic critical behaviour is suppressed near the QPT. The μSR results of phase separation and suppression of critical dynamics in $(Sr_{1-x}Ca_x)RuO_3$ exhibit a striking resemblance to those in MnSi, which suggests that these features may be generic to QPTs in itinerant ferromagnets/helimagnets.

We now explore quantum crossover behaviours from magnetically ordered (or superconducting) to disordered states in other correlated electron systems. Table 1 lists known cases in which the crossover is associated with either a first-order transition, phase separation or partial volume fraction of the ordered region. Note that volume-integrated measurements, such as bulk magnetization or neutron scattering, allow distinction of first-order transition only when an abrupt change is detected at the phase boundary. A continuous change in these measurements can be either due to a true second-order phase transition or to a first-order transition accompanied by phase separation, where the product of moment size and volume fraction exhibits a continuous variation as in Fig. 3d. In contrast, NMR/nuclear quadrupole resonance (NQR) and μSR can distinguish signals from ordered and disordered volumes. When single-crystal specimens are available, μSR has

the further advantage of avoiding pressure/system heterogeneities in powderized specimens. As demonstrated in Table 1, many known cases of QPTs, not only in itinerant magnets but also in heavy-fermion and high-$T_c$ systems, are associated with first-order transition/phase separation. It fact, it is not easy to find a well-established case of a QPT in such systems with a truly second-order transition.

In his pioneering theoretical contribution, which initiated modern discussions of QPT, Hertz[16] mapped the QPT to thermal counterparts in a higher effective dimension, where a better applicability of mean-field theory is expected. The issue of first- or second-order transition, related to specific materials conditions such as symmetry and ordering wavevector, was left open to subsequent studies. Figure 4 illustrates the evolution of the free energy as a function of the order parameter in typical second-order (lines 1 and 2) and first-order phase transitions (lines 3 and 4). Recently, Belitz *et al.*[17,18] ascribed first-order transitions in itinerant ferromagnets to terms in the free energy arising from coupling of low-energy spin fluctuation modes and order-parameter fluctuations, which leads to a free-energy profile similar to line 3 in Fig. 4 at $T_c$. Alternatively, first-order QPTs with such free-energy profiles may in general also be due to effects of band structure in metallic ferromagnets. Randomness would suppress low-energy fluctuations and/or smear out discontinuous changes, thus favouring a tendency towards an apparent second-order transition in both cases. The clear observation of phase separation in $(Sr_{1-x}Ca_x)RuO_3$, overcoming possible effects of randomness in chemically substituted systems, can then be taken as rather robust evidence against a second-order transition. Although first-order transition and phase separation are not necessarily identical concepts, they are associated with each other in the majority of cases. In general, when the relevant energy scale is lowered near a QPT, competing phenomena, such as superconductivity in $UGe_2$ and/or a generic tendency towards a first-order transition, become the dominant factors. This provides a natural way to understand the overwhelming tendency towards first-order transitions shown in Table 1.

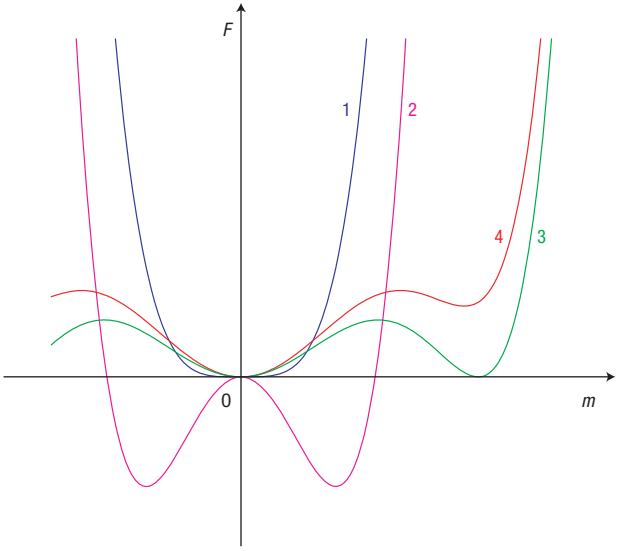


**Figure 4 Free-energy profile for the first- and second-order phase transitions.** A schematic view of the free energy, *F*, as a function of the magnetic order parameter, *m*, illustrated for a second-order phase transition in the disordered state (line (1)) and the ordered state (2), and a first-order phase transition at the ordering temperature or pressure (3) and in the disordered state near the ordering (4). A discussion for the situation with (3) in itinerant ferromagnets has been given, for example, by Belitz *et al.*[17,18].

**Table 1 Phase separation (PS)/first-order transition (FOT)/partial-volume (PVF) features detected at QPT.**

| System | Crossover | Parameter ($p$ in kbar) | FOT/PS/PVF | Method | Refs | Remark, [Limitation] |
|---|---|---|---|---|---|---|
| Itinerant electron magnets | | | | | | |
| $UGe_2$ | FM1–para | $p_c = 16$ | FOT | Magnetization | 27 | Sudden drop |
| | | | PS | Ge NQR | 28 | Coexisting signal (powder) |
| $ZrZn_2$ | FM–para | $p_c = 16.5$ | FOT | Magnetization | 29 | Sudden drop |
| MnSi | Helical–para | $12 = p^* < p < p_c = 14.6$ | FOT | Susceptibility | 1 | Sharp change |
| | | $p < p_c$ | FOT | Si NMR | 7 | (powder) |
| | | $p < 18$ | PVF | Si NMR | 8 | Intensity drop (powder) |
| | | $p^* < p < p_c$ | PS | μSR | Present work | Volume fraction, x-tal |
| | | | FOT | | | Suppressed critical dynamics |
| $(Sr_{1-x}Ca_x)RuO_3$ | FM–para | $0.7 < Ca(x) < 0.65$ | PS | μSR | Present work | Volume fraction |
| | | | FOT | | | Suppressed critical dynamics |
| Heavy-fermion systems | | | | | | |
| $CeCu_{2.2}Si_2$ | AF(a)–SC | Temp. | PS | μSR | 30 | AF volume change at SC |
| $URu_2Si_2$ | AF–hidden | $3 < p < 10$ | PVF | Si NMR | 31 | [hidden order missing] |
| | | $0 < p < 10$ | PVF/FOT | μSR | 32,33 | |
| $CeIn_3$ | AF–SC | $p_c = 24.3$ | FOT | In NQR | 34 and refs therein | FOT in AF–Para |
| High-$T_c$ systems | | | | | | |
| $(La, Sr)_2(Cu_{1-x}Zn_x)O_4$ | SC–normal | $Zn(x)$ | PS | μSR | 35 | Swiss Cheese model |
| $Bi_2Sr_2Ca(Cu_{2-x}Zn_x)O_8$ | SC–fnormal | $Zn(x)$ | PS | STM | 36 | Normal region around Zn |
| $(La_{1.85-y}Sr_{0.15}Eu_y)CuO_4$ | Stripe–SC | $Eu(y)$ | PS | μSR | 37 | Volume fraction trade-off |
| O-doped $(La_{2-x}Sr_x)CuO_{4+y}$ | Stripe–SC | Temp., $Sr(x)$ | PVF/PS | μSR | 10,38 | Stripe islands[10] |
| $Tl_2Ba_2CuO_{6+\delta}$ | SC–metal | Overdope $O(\delta)$ | PS | μSR | 24,39 | Boson–fermion coexistence |
| $Bi_2Sr_2CaCu_2O_{8+\delta}$ | SC–metal | Overdope $O(\delta)$ | PS | STM | 40 | Inhomogeneous gap closing |

FM: ferromagnetic, AF: antiferromagnetic, SC: superconducting phase, STM: Scanning tunnelling microscope.

As a novel type of spin correlation at a QPT, the partial-order correlations of MnSi have become a focus of theoretical interest, and several different models have been presented for their explanation, such as 'helical spin crystals'[19], 'blue quantum fog'[20] and 'skyrmion states'[21], as well as 'magnetic rotons'[22]. The magnetic-roton model views the partial-order correlations as a manifestation of a soft spin mode towards helical spin order, analogous to rotons in superfluid He, which crosses over to solid helium with increasing pressure at $p \sim 26$ bar via a first-order QPT[23]. These correlations may also be analogous to the 41 meV neutron resonance mode in the cuprate systems[24,25] heading towards the stripe spin/charge ordered state. By revealing the dynamic nature of the partial-order correlations, and providing their energy/timescale $10^{10-11}\,\mathrm{s}^{-1}$, the present results give severe constraints to future development of these models/theories.

In summary, we have presented μSR studies on dynamic and static magnetic behaviour at the QPTs of MnSi and $(Sr,Ca)RuO_3$, which demonstrate spontaneous phase separation and suppression of dynamic critical behaviour. It is interesting to note that nearly identical spin responses are observed in MnSi, which involves low crystal symmetry and a Dyaloshinskii–Moriya interaction[26], and in $(Sr,Ca)RuO_3$ having higher symmetry and a ferromagnetic ground state. These findings, together with other known cases in heavy-fermion and cuprate systems, promote the development of a comprehensive understanding of QPTs in correlated electron systems that clarifies the role of first-order transitions.

## METHODS

In μSR (see ref. 9 for a recent review of μSR studies in topical subjects and technical aspects of μSR) in a transverse field, the time spectrum from a paramagnetic/non-magnetic specimen (and pressure cell) is given by

$$N(t) = N_0 \exp(-t/\tau_\mu)[1 + AG(t)\cos(\gamma_\mu H_{\mathrm{ext}} t + \phi)],$$

where $\tau_\mu = 2.2\,\mu\mathrm{s}$ is the muon lifetime, $\gamma_\mu = 2\pi \times 13.6\,\mathrm{kHz\,G^{-1}}$ is the gyromagnetic ratio of the muon spin, $A \sim 0.2$–$0.3$ is the initial asymmetry (constant for a given spectrometer/beamline condition), $G(t)$ is the relaxation function, $H_{\mathrm{ext}}$ is the magnitude of the static external field (plus Knight shift) at the muon site and $\phi$ is the initial phase of the precession that depends on the location of the counter. When some volume undergoes static magnetic order, producing a static internal field $H_{\mathrm{int}}$ at the muon site, the oscillation amplitude for the frequency $\gamma_\mu H_{\mathrm{ext}}$ is reduced. In the case of MnSi below $T_c$, where the vector sum of $H_{\mathrm{ext}}$ (=100 G) and $H_{\mathrm{int}}$ (≥900 G at $T \to 0$ and $p = 0$) has a wide spread (∼100 G or more) in magnitude, the oscillating signal from the magnetically ordered volume is depolarized within $t = 100$ ns or less. As a demonstration of the response from a para/non-magnetic volume, Fig. 1b shows the raw data $|AG(t)\cos(\gamma_\mu H_{\mathrm{ext}} t + \phi)|$, together with the 'envelope' $AG(t)$ obtained by dividing the data by the cosine function (we avoided plotting the time region where the cosine function is close to zero). By fitting the amplitude of this cosine signal, assuming a slowly decaying function for $G(t)$ (due mostly to nuclear dipolar fields), we obtained the fraction of muons stopped in the paramagnetic region of MnSi plus the non-magnetic pressure cell. The cell contribution was calibrated using the data at $T = 2.5$ K at ambient pressure, where the full volume of MnSi is known to undergo static order. Subtracting this cell amplitude, we obtained the precession amplitude of muons representing the 'paramagnetic volume fraction of MnSi', from which the plot in Fig. 2a was constructed. In ZF or LF μSR, the time histograms for the forward (F)/backward (B) counters are given as

$$N_{\mathrm{F/B}}(t) = N_{F_0/B_0} \exp(-t/\tau_\mu)[1 \pm AG(t)].$$

The relaxation function, $G(t)$, describes the time evolution of muon spin polarization from the initial value of $G(t = 0) = 1.0$. Full relaxation corresponds to $G(t) = 0$. For signals from multiple different regions, such as the cell and the specimen, $G(t)$ is decomposed into additive signals from different regions. In paramagnetic systems, the sample signal usually exhibits an exponential decay $\exp(-t/T_1)$, whereas in the ordered state in ZF, a damped oscillation of 2/3 of the asymmetry, added to a slow decay of 1/3 asymmetry representing muons at sites with the internal field from ordered moments parallel to the initial muon polarization, is observed, as seen in $G(t)$ for $x < 0.5$ at low temperatures in Fig. 3a. This 2/3:1/3 ratio depends on the crystal orientation for single-crystal specimens, as well as the ratio between the external and internal fields in LF. For the cubic crystal symmetry of MnSi, which has eight [111] spiral directions, however, we expect that a balanced random population of domain orientations at low/zero field would minimize the orientation effect, leading nearly to a 2:1 ratio similar to the case for powder/ceramic samples. The asymmetry plotted in Fig. 2b corresponds to the relative magnitude of the non-oscillating component within the signal from the MnSi specimen, after the background signal from the pressure cell was subtracted.

Received 21 September 2006; accepted 2 November 2006; published 24 December 2006.

## References


1. Pfleiderer, C., McMullan, G. J., Julian, S. R. & Lonzarich, G. G. Magnetic quantum phase transition in MnSi under hydrostatic pressure. *Phys. Rev. B* **55**, 8330–8338 (1997).
2. Pfleiderer, C. *et al.* Partial order in the non-Fermi-liquid phase of MnSi. *Nature* **427**, 227–231 (2004).
3. Pfleiderer, C. *et al.* Coexistence of superconductivity and ferromagnetism in the d-band metal $ZrZn_2$. *Nature* **412**, 58–61 (2001).
4. Saxena, S. S. *et al.* Superconductivity on the border of itinerant-electron ferromagnetism in $UGe_2$. *Nature* **406**, 587–592 (2000).
5. Ishikawa, Y., Shirane, G., Tarvin, J. A. & Kohgi, M. Magnetic excitations in the weak itinerant ferromagnet MnSi. *Phys. Rev.* **B16**, 4956–4970 (1977).
6. Moriya, T. *Spin Fluctuations in Itinerant Electron Magnetism* vol. 56 (Springer Series in Solid State Science, Springer, Heidelberg, 1985).
7. Thessieu, C., Kitaoka, Y. & Asayama, K. Magnetic quantum phase transition in MnSi. *Physica B* **259–261**, 847–848 (1999).
8. Yu, W. *et al.* Phase inhomogeneity of the itinerant ferromagnet MnSi at high pressures. *Phys. Rev. Lett.* **92**, 086403 (2004).
9. Lee, S. L., Kilcoyne, S. H. & Cywinski, R. (eds) *Muon Science: Muons in Physics, Chemistry and Materials* (Inst. of Physics Publishing, Bristol, 1999).
10. Savici, A. T. *et al.* Muon spin relaxation studies of incommensurate magnetism and superconductivity in stage-4 $La_2CuO_{4.11}$ and $La_{1.88}Sr_{0.12}CuO_4$. *Phys. Rev. B* **66**, 014524 (2002).
11. Hayano, R. S. *et al.* Observation of the $T/(T - T_c)$ divergence of the $\mu^+$ spin-lattice relaxation rate in MnSi near $T_c$. *Phys. Rev. Lett.* **41**, 1743–1746 (1978).
12. Kadono, R., Matsuzaki, T., Yamazaki, T., Kreitzman, S. R. & Brewer, J. H. Spin dynamics of the itinerant helimagnet MnSi studied by positive muon spin relaxation. *Phys. Rev. B* **42**, 6515–6522 (1990).
13. Gat-Malureanu, I. M. *et al.* Field dependence of the muon spin relaxation rate in MnSi. *Phys. Rev. Lett.* **90**, 157201 (2003).
14. Kiyama, T., Yoshimura, K., Kosuge, K., Mitamura, H. & Goto, T. High-field magnetization of $Sr_{1-x}Ca_xRuO_3$. *J. Phys. Soc. Japan* **68**, 3372–3376 (1999).
15. Yoshimura, K. *et al.* $^{17}O$ NMR observation of universal behavior of ferromagnetic spin fluctuations in the itinerant magnetic system $Sr_{1-x}Ca_xRuO_3$. *Phys. Rev. Lett.* **83**, 4397–4400 (1999).
16. Hertz, J. A. Quantum critical phenomena. *Phys. Rev. B* **14**, 1165–1184 (1976).
17. Belitz, D., Kirkpatrick, T. R. & Vojta, T. First order transitions and multicritical points in weak itinerant ferromagnets. *Phys. Rev. Lett.* **82**, 4707–4710 (1999).
18. Belitz, D., Kirkpatrick, T. R. & Rollbühler, J. Tricritical behavior in itinerant quantum ferromagnets. *Phys. Rev. Lett.* **94**, 247205 (2005).
19. Binz, B., Vishwanath, A. & Aji, V. Theory of the helical spin crystal: A candidate for the partially ordered state of MnSi. *Phys. Rev. Lett.* **96**, 207202 (2006).
20. Tewari, S., Belitz, D. & Kirkpatrick, T. R. Blue quantum fog: Chiral condensation in quantum helimagnets. *Phys. Rev. Lett.* **96**, 047207 (2006).
21. Rössler, U. K., Bogdanov, A. N. & Pfleiderer, C. Spontaneous skyrmion ground states in magnetic metals. *Nature* (2006) (in the press) <http://www.arxiv.org/cond-mat/0603103>.
22. Schmalian, J. & Turlakov, M. Quantum phase transitions of magnetic rotons. *Phys. Rev. Lett.* **93**, 036405 (2004).
23. Dietrich, O. W., Graf, E. H., Huang, C. H. & Passell, L. Neutron scattering by rotons in liquid helium. *Phys. Rev. A* **5**, 1377–1391 (1972).
24. Uemura, Y. J. Condensation, excitation, pairing, and superfluid density in high-$T_c$ superconductors: Magnetic resonance mode as a roton analogue and a possible spin-mediated pairing. *J. Phys. Condens. Matter* **16**, S4515–S4540 (2004).
25. Uemura, Y. J. Twin spin/charge roton mode and superfluid density: Primary determining factors of $T_c$ in high-$T_c$ superconductors observed by neutron, ARPES, and MuSR. *Physica B* **374/375**, 1–8 (2006).
26. Bak, P. & Jensen, M. H. Theory of helical magnetic structures and phase transitions in MnSi and FeGe. *J. Phys. C: Solid State Phys.* **13**, L881–L885 (1980).
27. Pfleiderer, C. & Huxley, A. D. Pressure dependence of the magnetization in the ferromagnetic superconductor $UGe_2$. *Phys. Rev. Lett.* **89**, 147005 (2002).
28. Harada, A. *et al.* Cooperative phenomenon of ferromagnetism and unconventional superconductivity in $UGe_2$: A $^{73}Ge$-NQR study under pressure. *J. Phys. Soc. Japan* **74**, 2675–2678 (2005).
29. Uhlarz, M., Pfleiderer, C. & Hayden, S. M. Quantum phase transitions in the itinerant ferromagnet $ZrZn_2$. *Phys. Rev. Lett.* **93**, 256404 (2004).
30. Luke, G. M. *et al.* Competition between magnetic order and superconductivity in $CeCu_{2.2}Si_2$. *Phys. Rev. Lett.* **73**, 1853–1856 (1994).
31. Matsuda, K., Kohori, Y., Kohara, T., Kuwahara, K. & Amitsuka, H. Spatially inhomogeneous development of antiferromagnetism in $URu_2Si_2$: Evidence from $^{29}Si$ NMR under pressure. *Phys. Rev. Lett.* **87**, 087203 (2001).
32. Luke, G. M. *et al.* Muon spin relaxation in heavy fermion systems. *Hyperfine Interact.* **85**, 397–409 (1994).
33. Amitsuka, H. *et al.* Hidden order and weak antiferromagnetism in $URu_2Si_2$. *Physica B* **312/313**, 390–396 (2002).
34. Kitaoka, Y., Kawasaki, S., Mito, T. & Kawasaki, Y. Unconventional superconductivity in heavy fermion systems. *J. Phys. Soc. Japan* **74**, 186–199 (2005).

35. Nachumi, B. *et al.* Muon spin relaxation studies of Zn-substitution effects in high-$T_c$ cuprate superconductors. *Phys. Rev. Lett.* **77**, 5421–5424 (1996).
36. Pan, S. H. *et al.* Imaging the effects of individual zinc impurity atoms on superconductivity in $Bi_2Sr_2CaCu_2O_{8+\delta}$. *Nature* **403**, 746–750 (2000).
37. Kojima, K. M. *et al.* Superfluid density and volume fraction of static magnetism in stripe-stabilized $La_{1.85-y}Cu_ySr_{0.15}CuO_4$. *Physica B* **326**, 316–320 (2003).
38. Mohottala, H. E. *et al.* Phase separation in superoxygenated $La_{2-x}Sr_xCuO_{4+y}$. *Nature Mater.* **5**, 377–382 (2006).
39. Uemura, Y. J. *et al.* Magnetic field penetration depth in $Tl_2Ba_2CuO_{6+\delta}$ in the overdoped regime. *Nature* **364**, 605–607 (1993).
40. Slezak, J. A. Scanning tunneling spectroscopy studies of $Bi_2Sr_2CaCu_2O_{8+x}$ from the strongly underdoped to strongly overdoped regime. in *APS March Meeting, Baltimore, 2006*, online abstract in <http://meetings.aps.org/Meeting/MAR06/Event/42945>.

## Acknowledgements

We acknowledge financial support from NSF DMR-05-02706 (Material World Network, Inter-American Materials Collaboration program) at Columbia and Kentucky, NSF DMR-01-02752 and CHE-01-11752 at Columbia, NSERC and CIAR (Canada) at McMaster, Brazilian grant CIAM-CNPq 49.2674/2004-3 at CBPF and CIAM-CONICET project 509/20-04-05 at CAB Bariloche, Argentina; technical support from S.R. Kreitzman and K. Satoh and scientific discussions with B. Binz, M. Continentino, S.R. Julian and A.J. Millis.
Correspondence and requests for materials should be addressed to Y.J.U.

## Competing financial interests

The authors declare that they have no competing financial interests.